

The Role of Wakes in the Mechanism of Extraction in Spray Columns

EPHRAIM KEHAT and RUTH LETAN

Technion, Israel Institute of Technology, Haifa, Israel

Extraction in spray columns is reexamined in view of recent information on wakes of drops and the role of wakes in the mechanism of heat transfer in spray columns. In the proposed mechanism, mass is extracted from a highly mixed drop to a highly mixed wake in the wake growth zone. Elements of wakes are shed, mixed with continuous phase, and are replaced by the continuous phase in the wake shedding zone. A narrow mixing zone exists at the entrance of the continuous phase and above it the coalescence zone.

A mathematical model for extraction in spray columns is presented. This model was used to calculate the top concentrations from the bottom concentrations, for 258 runs from nine papers covering very wide ranges of columns, systems, and operation parameters. Better than 20% agreement was obtained for 100 runs and the poorer agreement of most other runs can be attributed to the sensitivity of the calculations to the uncertainties in the average distribution coefficients of the solute between the two liquid phases, and, to a lesser extent, to the uncertainties in the length of the wake shedding zone and wake parameters. For very large or very small values of the distribution coefficient, the assumption of local equilibrium between drop and wake, used in the model, does not hold.

Commercial extraction is rarely conducted in spray columns. Morello and Poffenberger (23) surveyed the commercial extraction equipment in use in 1950. Of the 47 systems covered only two used spray columns. Hanson (11) recently has attributed the nonuse of extraction spray columns to their inefficiency, due to the massive backmixing in the continuous phase.

Spray columns have some attractive advantages over other equipment: low cost, simplicity of mechanical design, high throughputs, and relative insensitivity to accumulation of dirt. However, despite the voluminous literature on extraction in spray columns (1, 3 to 10, 13 to 16, 25, 26, 28 to 30), it is not possible to correlate the data for more than one system or to design a large spray column from laboratory data.

Recently, we have discussed the mechanics of spray columns (18) and we have suggested (19) a new mechanism for heat transfer in a spray column heat exchanger, based on the role on the wakes of the drops. This mechanism showed good agreement with experimental temperature profiles (19). The key to the mechanism was the temperature profiles close to the dispersion nozzles. The temperature of the dispersed phase changed with distance from the dispersion nozzles, while the temperature of the continuous phase remained constant in this region. The only place where the heat lost or gained by the drops could be accumulated is in the wakes of the drops, as the wakes are formed.

Concentration profiles measured in an extraction spray column by Gier and Hougen (10) showed a similar phenomenon. A concentration change of the dispersed phase above the dispersion plate, with no corresponding change in the continuous phase, were noted. Cavers and Ewan-chyna (3) also noted that a material balance could not be made for the two phases for any position within the column, and attributed this effect to "envelopes" of the continuous phase carried with the dispersed phase up the column, discharging at the coalescence interface and moving back down the column. Substitution of "wakes" for "envelopes" would come close to the actual mechanism.

Garner and Tayeban (7) were the first to state the need to consider the role of wakes in extraction spray columns. They postulated that solute diffuses very slowly from drop to wake and from wake to continuous phase, or vice versa.

Literature on wakes of drops has proliferated recently. Magarvey and Bishop (21) observed and classified the wakes behind single liquid drops falling through quiescent water, and noted the approximate ranges of Reynolds numbers corresponding to transition from one wake configuration to the next. They observed that wake shedding starts at about Reynolds numbers of 360. In a later paper Magarvey and Maclatchy (22) noted that shed vortex elements from the wake carry material to the continuous phase by periodic escape of short vorticity bursts or shed vortex loops, that vortex loop elements are built up and shed alternately from opposite sides of the drop axis, and that the rate at which mass is transferred from the drop to the ambient fluid is not very great during the period in which the wake is being established behind the drop.

Hendrix et al. (12) measured the size of the wakes of single drops of a number of organic liquids rising in quiescent water. The relative wake to drop size, calculated from their data, increases with drop size, up to the drop size range, where oscillations of drops started. Winnikow and Chao (32) found that the onset of oscillation coincided with the onset of periodic shedding of vortices from the wakes. Magarvey and Maclatchy (22) observed that the frequency of oscillations is equal to the frequency of wake shedding. Baird et al. (2) showed that induced oscillations increase the rate of wake shedding.

In this work a mathematical model for the extraction in spray column that emphasizes the role of wakes in the extraction mechanism, which is generally similar to the model developed earlier for the mechanism of heat transfer in a spray column (19), is presented. This model was applied to the data of 258 runs from nine papers with very severe restrictions. The results show that the wake model can be applied successfully to extraction in spray columns.

THE PHYSICAL MODEL

The physical model is similar to the one presented in detail for heat transfer (19). The prominent features of this model are reviewed here. For convenience, mass transfer from drops to continuous phase and a dispersed packing of drops of lower density than the continuous phase is described.

The drop is formed by the breakup of a liquid jet of the dispersed phase. Continuous phase liquid at the outlet concentration passes through the boundary layer of highly mixed drops into the highly mixed wake as the wake is formed and grows. This liquid extracts solute from the drop at a rate high enough to reach local equilibrium with the drop. (This is the most extreme assumption in this model. When this assumption is not justified, another parameter, the local rate of mass transfer, should be considered.) The intermediate region observed for some temperature profiles, in which the temperature of both phases was constant (19), was not observed for concentration profiles (3, 9, 10) and is negligible for mass transfer.

Above the wake growth zone, the drops and wakes enter the wake shedding zone. In this zone, wake shedding and mixing of the shed wake elements with the continuous phase take place. New continuous phase liquid replaces the material lost from the wakes, after extracting solute at local equilibrium with the drops.

At the entrance of the continuous phase, the liquids pass through a mixing zone (17), into which flow drops and their wakes, continuous phase and shed wakes from the coalescence zone. At the coalescence zone the wakes are shed completely and the liquid of the wakes returns to mix with the continuous phase in the mixing zone.

THE MATHEMATICAL MODEL

The following assumptions are made: steady state, constant average properties of the two liquids, constant average distribution coefficient, constant average drop size and holdup, plug flow of the drops, dispersed packing of drops, and a constant rate of shedding and size of wake in the wake shedding zone.

Wake Growth Zone

The concentration of the solute in the continuous phase is constant in this zone. The drop is perfectly mixed. Elements of the continuous phase in contact with the drop reach an equilibrium concentration with the drop on their way to the forming, fully mixed wake

$$C_c^* = \frac{C_d}{K} \quad (1)$$

Mass balance on the drop (Figure 1a) gives

$$(C_{co} - C_c^*) dM_D = v_D dC_d \quad (2)$$

Elimination of C_c^* from Equation (2) by Equation (1) and integration of Equation (2) over the wake growth zone give

$$M = K \ln \left[\frac{C_{di}/K - C_{co}}{C_{ds}/K - C_{co}} \right] \quad (3)$$

The concentration of the solute in the drop at the top of this zone is obtained from Equation (3) in the form of

$$\frac{C_{ds}}{K} = \left(\frac{C_{di}}{K} - C_{co} \right) \exp \left(-\frac{M}{K} \right) + C_{co} \quad (4)$$

An overall mass balance for drop and wake in this zone gives

$$M_D (C_{ws} - C_{co}) = v_D (C_{di} - C_{ds}) \quad (5)$$

The concentration of solute in the wake at the top of the wake growth zone is found by combining Equations (4) and (5) to eliminate C_{ds} :

$$C_{ws} = \frac{K}{M} \left(\frac{C_{di}}{K} - C_{co} \right) \left[1 - \exp \left(-\frac{M}{K} \right) \right] + C_{co} \quad (6)$$

Wake Shedding Zone

The variable distance in this zone is z and changes from zero to l , the length of the wake shedding zone. This is

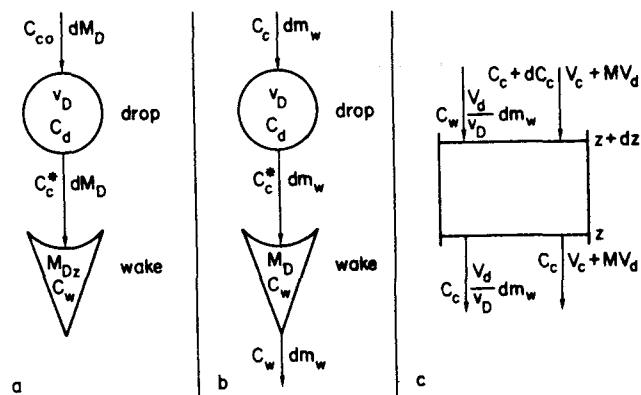


Fig. 1. (a) Mass transfer in the wake growth zone. Mass transfer in the wake shedding zone; (b) for the drop and wake; (c) for the continuous phase.

the only zone length which changes with change of column length (L).

Mass balance on the drop (Figure 1b) gives

$$(C_c - C_c^*) dm_w = v_D dC_d \quad (7)$$

Elimination of C_c^* by Equation (1) and dividing by dz results in

$$\frac{dC_d}{dz} + m \left(\frac{C_d}{K} - C_c \right) = 0 \quad (8)$$

where, by the assumption of a constant rate of wake shedding

$$m = \frac{1}{v_D} \frac{dm_w}{dz} \quad (9)$$

Mass balance on the wake (Figure 1b) gives

$$(C_c^* - C_w) dm_w = M_D dC_w \quad (10)$$

which, by the same procedure used before, yields

$$\frac{dC_w}{dz} + \frac{m}{M} \left(C_w - \frac{C_d}{K} \right) = 0 \quad (11)$$

Mass balance on the continuous phase (Figure 1c) takes into account the returning wakes from the coalescence zone (MV_d):

$$(V_c + MV_d) dC_c = V_d (C_c - C_w) \frac{dm_w}{v_D} \quad (12)$$

where $V_d \frac{dm_w}{v_D}$ is the amount of wake contents that is exchanged in the differential volume.

Division by dz yields

$$\frac{dC_c}{dz} + \frac{m}{P} (C_w - C_c) = 0 \quad (13)$$

where

$$P = \frac{V_c + MV_d}{V_d} = \frac{1}{R} + M \quad (14)$$

and

$$R = V_d/V_c \quad (15)$$

Equations (8), (11), and (13) can be solved simultaneously with the boundary conditions at $z = 0$: $C_d = C_{di}$, $C_w = C_{ws}$, $C_c = C_{co}$. C_{ds} and C_{ws} can be obtained in terms of the bottom concentrations C_{di} and C_{co} from Equations (4) and (6).

The concentration profiles of the drops, continuous phase, and wakes in the wake shedding zone are given in a

dimensionless form by Equations (16) to (18):

$$\Theta_d = \frac{\frac{C_d}{K} - C_{co}}{\frac{C_{di}}{K} - C_{co}} = \left\{ \frac{m}{K} \left[\frac{1+S}{\alpha_1} \{1 - \exp(\alpha_1 z)\} - \frac{S}{\alpha_2} \{1 - \exp(\alpha_2 z)\} \right] + 1 \right\} \exp\left(-\frac{M}{K}\right) \quad (16)$$

$$\Theta_c = \frac{\frac{C_c}{K} - C_{co}}{\frac{C_{di}}{K} - C_{co}} = \left\{ \frac{m}{K} \left[\frac{1+S}{\alpha_1} \left[1 - \left(\frac{K}{m} \alpha_1 + 1 \right) \exp(\alpha_1 z) \right] - \frac{S}{\alpha_2} \left[1 - \left(\frac{K}{m} \alpha_2 + 1 \right) \exp(\alpha_2 z) \right] \right] + 1 \right\} \exp\left(-\frac{M}{K}\right) \quad (17)$$

$$\Theta_w = \frac{\frac{C_w}{K} - C_{co}}{\frac{C_{di}}{K} - C_{co}} = \left\{ \frac{m}{K} \left[\frac{1+S}{\alpha_1} \left[1 - \left(\frac{K}{m} \alpha_1 + 1 \right) \exp(\alpha_1 z) \right] \times \left(1 - \frac{P}{m} \alpha_1 \right) \exp(\alpha_1 z) - \frac{S}{\alpha_2} \left[1 - \left(\frac{K}{m} \alpha_2 + 1 \right) \exp(\alpha_2 z) \right] \times \left(1 - \frac{P}{m} \alpha_2 \right) \exp(\alpha_2 z) \right] + 1 \right\} \exp\left(-\frac{M}{K}\right) \quad (18)$$

where

$$\alpha_1 = -\frac{m}{2} \left[\left(\frac{1}{M} + \frac{1}{K} - \frac{1}{p} \right) + \sqrt{\left(\frac{1}{M} + \frac{1}{K} + \frac{1}{p} \right)^2 - \frac{4}{MK}} \right] \quad (19a)$$

$$\alpha_2 = -\frac{m}{2} \left[\left(\frac{1}{M} + \frac{1}{K} - \frac{1}{p} \right) - \sqrt{\left(\frac{1}{M} + \frac{1}{K} + \frac{1}{p} \right)^2 - \frac{4}{MK}} \right] \quad (19b)$$

and

$$S = \frac{\alpha_1 + \frac{m}{K} - \frac{Km}{PM} \left[\exp\left(\frac{M}{K}\right) - 1 \right]}{\alpha_2 - \alpha_1} \quad (20)$$

Equations (16) to (18) are identical to Equations (16) to (18) for heat transfer (19) if K is substituted for r , C_d/K for t_d , C_{di}/K for t_{di} , and C for t in all cases.

Mixing Zone

All streams leaving the mixing zone are at equilibrium and therefore

$$C_{do} = K C_{cl} \quad (21)$$

Mass balance around the whole column gives

$$V_d(C_{di} - C_{do}) = V_c(C_{co} - C_{ci}) \quad (22)$$

which, when combined with Equation (21), yields

$$C_{ci} = C_{co} - RK \left(\frac{C_{di}}{K} - C_{cl} \right) \quad (23)$$

C_{cl} can be calculated from Equation (17) at $z = l$. The top concentrations C_{do} and C_{ci} can be calculated from Equations (17), (21), and (23) and the specified concentrations at the bottom of the column.

PARAMETRIC ANALYSIS OF THE MATHEMATICAL MODEL

For any set of bottom concentrations, the top concentrations are a function of the length of the wake shedding zone (l) and four parameters: the distribution coefficient (K), the ratio of flow rates of the two liquids (R), the relative wake size (M), and the relative rate of wake shedding (m). Essentially, the usual overall mass transfer coefficient or the height of a transfer unit is replaced by the two wake parameters.

The effect of the ratio of flow rates and the distribution coefficient for one column and one set of wake parameters and bottom concentrations on one top concentration [the other top concentration is easily available by Equation (22)] is plotted in Figure 2. For this set of bottom concentrations, the top concentration increases with increase of R for $K > 0.5$, does not change for $K = 0.5$, and decreases with increase of R for $K < 0.5$.

It is possible to generalize this plot for any bottom concentrations by plotting the dimensionless concentration Θ_b against the varying parameters, where

$$\Theta_b = \frac{C_{di} - C_{do}}{C_{di}/K - C_{co}} \quad (24)$$

Figures 3 to 6 are plots of Θ_b as function of the following combinations of parameters: K and R , RK and R , l and R , M and m , and can be used for evaluation of the effects of these parameters for any system. Since Θ_b includes K directly and R indirectly (through the material balance, only Figure 6, for which these two parameters do not vary, can be used for generalized comments.

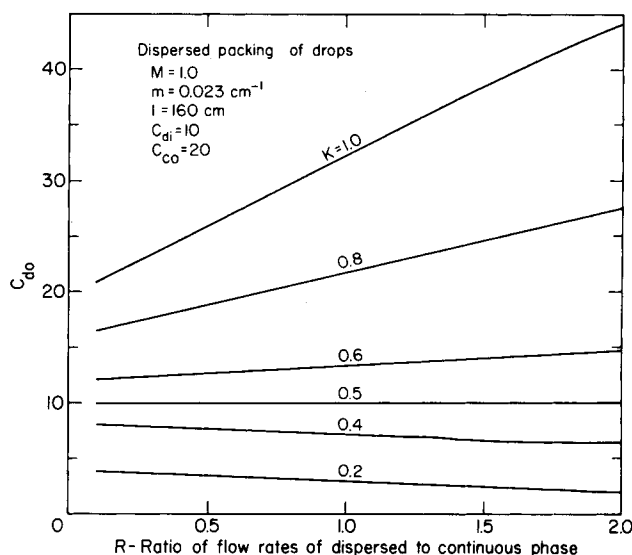


Fig. 2. Variation of the top concentration as function of R and K .

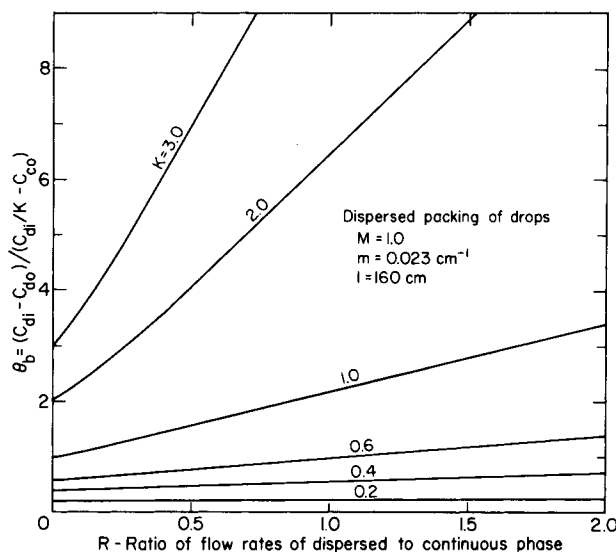


Fig. 3. Θ_b as function of R and K .

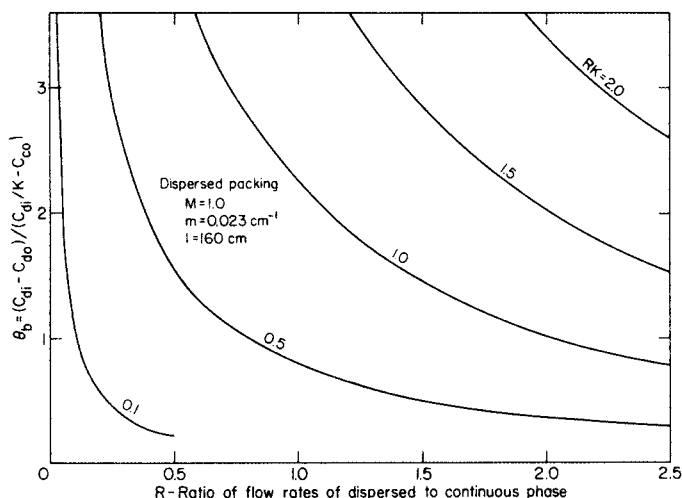


Fig. 4. θ_b as function of R and RK .

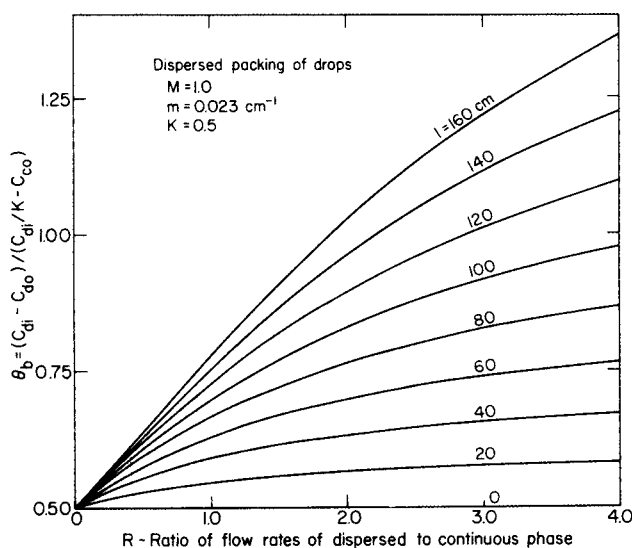


Fig. 5. θ_b as function of R and l .

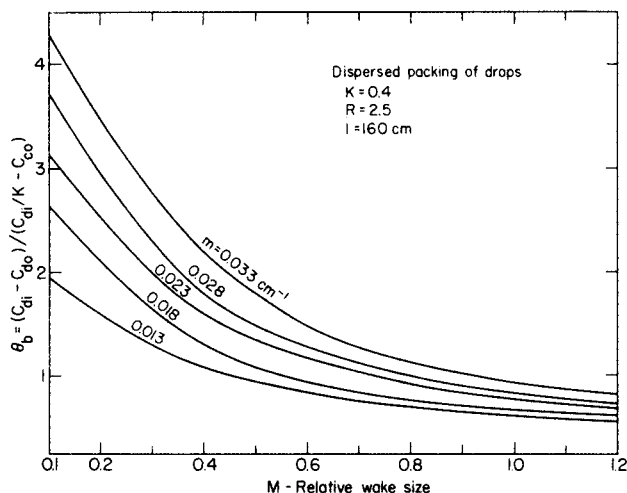


Fig. 6. θ_b as function of M and m .

Combination of Equations (22) and (24) gives

$$\theta_b = \frac{K}{R} \frac{C_{co} - C_{ci}}{C_{di} - KC_{co}} \quad (25)$$

For constant K and R , θ_b is the concentration change of the continuous phase in the column divided by the bottom driving force. From Figure 6, θ_b increases with increase of m and decrease of M , that is, with an increased number of exchanges of the wake contents up the column.

For the particular case of $RK = 1$, the driving forces at the bottom and top of the column are equal. The material balance, Equation (22), can be written as

$$R(C_{di} - C_{do}) = C_{co} - C_{ci} \quad (26)$$

By multiplying this equation by K , introducing $RK = 1$, and rearranging, we obtain

$$C_{di} - KC_{co} = C_{do} - KC_{ci} \quad (27)$$

For this particular case, θ_b is related to the number of transfer units calculated from the end concentrations, since the driving forces at both ends of the column are equal. Therefore

$$NTU = \int_L \frac{dC_d}{C_d - KC_c} = \frac{C_{di} - C_{do}}{C_{di} - KC_{co}} = \frac{\theta_b}{K} \quad (28)$$

From Figure 6, which was calculated for $RK = 1$, we can see that the number of transfer units increases with an increased number of exchanges of the wake contents up the column.

APPLICATION OF THE MATHEMATICAL MODEL TO EXPERIMENTAL DATA

Most of the data in the literature are in the form of performance coefficients. Nine papers in which single-component solvents were used and which report inlet and outlet compositions were found in the literature. Of the 261 runs in these papers only three runs, from Gier and Hougen (10), for which the effective column height was not available could not be used.

Details of the columns and nozzles used in these papers are summarized in Table 1. Column diameters ranged from 3.6 to 15.4 cm. and column heights from 15.3 to 160 cm. Nozzle diameters did not vary much, from 2.29 to 3.2 mm. Typically, drop sizes were not reported in any paper, and only two papers report drop holdup in the range of 3 to 24%. In some cases operation was in the flooding, or dense packing, range (18). However most runs were in the dispersed packing range.

Table 2 summarizes the range of system and operating parameters. Twenty-five sets of runs cover seven experimental systems, although about half the runs are for the M.I.K-acetic acid-water system. Water was one of the solvents for all runs. Either solvent was dispersed and either direction of extraction was used. Distribution coefficients varied from 0.014 to 55.5. The ratio of flow rates of dispersed to continuous phase was 0.143 to 10.8. Inlet concentrations ranged from 0 to 76.5×10^{-3} lb.-mole/cu. ft. for the dispersed phase and from 0 to 143.3×10^{-3} lb.-mole/cu. ft. for the continuous phase. All runs were conducted at room temperature over a narrow temperature range.

The length of the wake shedding zone was required for the analysis and only the effective distance between the inlets of the two phases was given for the experimental data. Garner and Tayeban (7) suggest that the length of the wake growth zone is 17 to 18 cm. Our temperature profiles (19) indicate a range of 10 to 35 cm. at low holdups. The concentration profiles (9, 10, 14, 30) indicate that the lengths of the mixing zone for these studies were about 0 to 10 cm. Therefore l probably ranged from $(L-10)$ to $(L-45)$ cm.

Concentration profiles measured experimentally (3, 9, 10) may not represent the true concentration profiles, since during the sampling process, wakes are caught with drops and continuous phase, and wake breakup and mixing with continuous phase can take place.

TABLE 1. DETAILS OF COLUMNS AND NOZZLES USED FOR THE ANALYZED DATA

Paper and reference	No. of sets	No. of runs	Columns		Nozzles	
			Height, cm.	Diameter, cm.	Number	Diameter, cm.
Elgin and Browning (5)	4	47	124.5	5.2		(3.16)
Geankoplis, Wells, and Hawk (9)	1	12	160	9.6	19-73	2.55
Gier and Houghton (10)	1	6	100.6-152.5	15.4	113	2.4
Kreager and Geankoplis (14)	1	19	15.3-91.5	3.6	4-11	2.55
Vogt and Geankoplis (31)	3	30	15.3-91.5	3.6, 3.88	4-11	2.55
Fleming and Johnson (6)	2	6	75	5.1	21, 56	2.56
Sherwood, Evans, and Longcor (28)	2	7	154-160	9.0	60	3.06
Johnson and Bliss (13)	9	109	60.5-109	5.2	9-36	2.29-3.2
Cavers and Ewanchyna (3)	2	22	107-110	3.95	10, 21	2.55
Range	9	25	258	15.3-160	4-73	2.29-3.2

TABLE 2. RANGE OF VARIABLES FOR THE ANALYZED DATA AND AVERAGE DEVIATION OF THE PROPOSED MODEL FROM THE EXPERIMENTAL DATA

Ref.	Set	No. of runs	Dispersed phase	Continuous phase	Solute	Direc- tion of extrac- tion	Inlet concentration, 10 ³ × lb.-mole/cu. ft.		Dispersed phase	Continuous phase e	R	K	Source of K	Average devia- tion %
(5)	1	18	Isopropyl ether	Water	Acetic acid	c	d	0.4 - 3.9	20.9 -143.3	0.333- 1.62	0.187-0.239	(5)	5.45	
	2	6	Water	Isopropyl ether	Acetic acid	d	c	65.6 -67.4	1.0 - 1.3	0.871- 2.32	4.88 -4.95	(5)	78.80	
	3	16	Isopropyl ether	Water	Acetic acid	d	c	5.7 -37.2	0.1 - 0.2	0.143- 1.93	0.176-0.187	(5)	10.88	
	4	7	Water	Isopropyl ether	Acetic acid	c	d	0.1	6.3 - 12.4	0.919- 3.17	5.2 -5.5	(5)	50.93	
(9)	5	12	Toluene	Water	Acetic acid	d	c	8.76-23.0	0.	0.332- 1.335	0.04 -0.062	(27)	48.03	
(10)	6	6	Diethyl ether	Water	Adipic acid	c	d	0. - 0.029	2.92- 3.01	0.5 - 1.47	0.513	(10)	22.20	
(31)	7	17	M.I.K.	Water	Propionic acid	d	c	10.12-30.43	0.	0.71 - 1.51	1.88 -1.99	(13)	212.14	
	8	8	M.I.K.	Water	Propionic acid	c	d	0.	9.64- 30.28	0.491- 1.27	1.90 -2.0	(13)	74.24	
	9	5	M.I.K.	Water	Formic acid	c	d	0.	6.73- 20.18	0.741- 1.27	0.412-0.422	(30)	27.46	
(14)	10	19	M.I.K.	Water	Propionic acid	c	d	0.	9.87- 30.5	0.509- 1.29	1.9 -2.01	(13)	84.12	
(6)	11	3	M.I.K.	Water	Acetic acid	c	d	0.	51.3	2.86 - 3.87	0.490-0.495	(6)	59.58	
	12	3	Water	M.I.K.	Acetic acid	c	d	0.	28.6	0.99 - 1.95	2.03 -2.07	(6)	325.73	
(28)	13	4	Benzene	Water	Acetic acid	c	d	0.01- 0.061	61.7 - 62.6	0.5 - 3.	0.018	(24)	110.33	
	14	3	M.I.K.	Water	Acetic acid	c	d	0.71- 1.13	56.4 - 60.7	0.45 - 1.	0.52 -0.54	(6)	5.25	
(13)	15	40	M.I.K.	Water	Acetic acid	d	c	0.	34.55- 75.8	0.23 - 4.16	0.48 -0.54	(6)	18.43	
	16	10	Water	M.I.K.	Acetic acid	d	c	48. -76.5	0.	0.94 - 3.55	1.87 -2.04	(6)	66.81	
	17	6	M.I.K.	Water	Acetic acid	d	c	38.24-29.6	0.	0.29 - 2.8	0.48 -0.9	(6)	39.48	
	18	27	Water	M.I.K.	Acetic acid	c	d	0.	25.64- 33.5	0.36 -10.8	2.02 -2.17	(6)	84.53	
	19	5	Water	M.I.K.	Propionic acid	c	d	0.	47. 48.	0.98 - 3.01	0.513-0.519	(13)	40.52	
	20	4	M.I.K.	Water	Propionic acid	c	d	0.	24.9 - 26.5	1.08 - 2.96	1.90 -1.94	(13)	23.91	
	21	3	Water	M.I.K.	Benzoic acid	c	d	0.	78.7 - 79.5	0.92 - 3.8	0.014	(13)	634.27	
	22	4	Benzene	Water	Acetic acid	d	c	51.4 -55.5	0.	0.99 - 3.95	55.5	(24)	4653.9	
	23	10	Water	Benzene	Acetic acid	c	d	0.	50.1 - 54.1	1.0 - 7.44	0.018	(24)	228.98	
(3)	24	17	M.I.K.	Water	Acetic acid	c	d	5.15- 7.84	44.4 - 53.3	0.43 - 5.3	0.49 -0.52	(6)	25.60	
	25	5	M.I.K.	Water	Acetic acid	d	c	11.82-14.54	0.04- 0.28	0.68 - 2.66	0.47 -0.48	(6)	27.17	
Total	25	258		7		2	0.	-76.5	0. -143.3	0.143-10.8	0.014-55.5			

For kerosene drops, 3 to 4 cm. in diameter, and low holdups, we found that the wake parameters for a wide range of flow rates and holdups were approximately $M = 1.0$ and $m = 0.023 \text{ cm.}^{-1}$ (19). Hendrix et al. (12) showed that the relative wake size is a function of drop size and system. Therefore other wake parameters were also used in the analysis.

Since a computer was used for the analysis of the experimental data, l , K , M , and m were varied over a wide range, and obviously with four parameters many combina-

tions were found that gave complete agreement for the theoretical equations for each run. From the results of this analysis it was difficult to decide which combination of parameters has a physical meaning.

In order to subject the theoretical equations to a more severe test, calculations were then made for all the experimental data for one combination of parameters: $M = 1.0$ and $m = 0.023$ for all runs and $l = L/30$ and one average value of K for each run. The top concentrations were calculated from the theoretical equations and the bottom experimental

TABLE 3. EFFECT OF VARIATIONS OF K AND l ON THE VALUES OF THE DEVIATION OF THE PROPOSED MODEL FROM THE EXPERIMENTAL DATA

Ref.	(5)					(13)					
Run	30	48	51	17	46	8	106				
1	K	dev.	K	dev.	dev.	K	dev.	dev.	K	dev.	dev.
$L \sim 30$	0.16	31.7	4.44	-73.1	-356.8	1.6	-373	23.8	0.4	23.6	13.4
$L \sim 30$	0.18	20.5	4.995	59.8	199.3	1.8	-216	13.9	0.45	13.2	0.4
$L \sim 30$	0.20	7.9	5.55	189.7	750.8	2.0	-58	4.0	0.5	3.1	-12.7
$L \sim 30$	0.22	-6.0	6.105	317.4	129.8	2.2	101	-5.8	0.55	-6.7	-25.7
$L \sim 30$	0.24	-21.4	6.6	443.0	184.2	2.4	259	-15.5	0.6	-16.0	-25.9
L	0.2	6.5	5.55	216.7	109.0	2.0	-126	-52.3	0.5	0.96	-30.6
$L \sim 30$	0.2	7.9	5.55	189.7	750.8	2.0	-58	4.0	0.5	3.1	-12.7
$L \sim 60$	0.2	9.9	5.55	168.6	526.3	2.0	-9	40.0	0.5	6.2	5.4

$M = 1.0$, $m = 0.023 \text{ cm.}^{-1}$

concentrations and compared with the top experimental concentrations by the equation

$$\text{deviation} = 100 \times \frac{C_{ci \text{ calc}} - C_{ci \text{ exp}}}{(C_{co} - C_{ci})_{\text{exp}}} \quad (29)$$

A similar equation for the dispersed phase gave different values only when the material balance for the original data was poor. The calculated top concentrations, the deviations, and the experimental data for all 258 runs are given in Table 4[†] Table 2 summarizes the average absolute values of the deviations for the continuous phase for each set of runs. The average deviation for the 25 sets of data range from 5.45 to 4654%. For 65 runs the deviation was less than 10% and for 35 runs the deviation was between 10 and 20%. In total, for 100 runs the deviation was less than 20%. For 20 runs with large deviations the material balance in the original data is very poor and for 17 runs with large deviations, short columns, 30.5 cm. or less in effective length, were used and the assumption of $l = L-30$ cannot hold.

For the three runs in set 22 with $K = 55.5$ the deviations are extremely high. For these runs the proposed model does not hold, since it assumes local equilibrium between drop and wake, and the large value of the distribution coefficient demands that all the mass transfer take place in the short wake growth zone. Similarly, for the 17 runs in sets 13, 21, and 23 with $K = 0.014$ to 0.018 , where the theoretical equations assume that most of the mass transfer takes place in the wake growth zone, the proposed model does not hold. For solute transfer from the dispersed to the continuous phase, coalescence of the dispersed phase within the column takes place for many systems. In these cases the values of the wake parameters would vary considerably along the column. This may possibly account for the generally poorer agreement of the theoretical model with experimental data of this type (Table 2). The deviations for the other runs are due to the uncertainties in the values of the distribution coefficient, the wake parameters, and the length of the wake shedding zone. Some idea about the magnitude of the effect of these uncertainties can be obtained from Table 3. For large K values a change in K of 10% can change the deviation from 0 to hundreds of percent. For lower values of K the effect of uncertainties in the values of K is smaller. The effect of variations in the values of l is very large for large values of K and is small for low values of K . The effect of variations in the values of the wake parameters is of the order of magnitude of the effect of l .

The same analysis was repeated for two other sets of

wake parameters. For $M = 1.0$ and $m = 0.03 \text{ cm.}^{-1}$, 96 runs with deviations smaller than 20% were obtained. For $M = 0.83$ and $m = 0.03 \text{ cm.}^{-1}$ (19), only 90 runs with deviations smaller than 20% were obtained.

CONCLUSIONS

In view of the severe test of the theoretical model in this study, by the use of one set of operating parameters, M , m , and $L-l$, and despite the variations in holdup, drop size, and initial drop velocities, it is remarkable that very good agreement was obtained for about 40% of experimental runs. Most deviations can be attributed to the effect of the variations of the actual parameters that were used in the calculations presented here.

For extreme values of the distribution coefficient, and for bottom concentrations which are far from equilibrium, the proposed model does not hold, since it is unlikely that local equilibrium between drop and wake can be achieved in the short wake formation zone.

Wakes of drops play an important role in the mechanism of extraction in spray columns. Other contacting equipment in which drops are contacted with continuous phase should also be examined to determine the role of the wakes in the mechanism of transfer.

Since the difference between l and L is negligible for long columns, and computing programs can be written to take into account the change of K along the column, it should be possible to design extraction spray columns accurately when more data become available for the wake parameters.

It was shown (18, 20) for heat transfer in spray columns that it is more advantageous to operate a spray column with a dense packing of drops. The length of an extraction spray column operating with a dense packing of drops would be considerably less than for operation with a dispersed packing of drops, which was used in all the studies of extraction spray columns. The use of a dense packing of drops would make commercial extraction in spray columns feasible.

NOTATIONS

C = solute concentration, lb.-mole/cu. ft.
 C_p = heat capacity, cal./g.(°C.)
 $K = C_d/C_c^*$ distribution coefficient between dispersed and continuous phases
 L = effective length of column, cm.
 l = length of wake shedding zone, cm.
 M = relative wake size = M_D/v_D
 M_D = wake volume, cc.
 m = volume of wake elements shed per volume of drop and unit distance traveled, cm.^{-1}
 m_w = volume of wake shed, cc.
 $P = (1 + MR)/R$

[†]Table 4 has been deposited as document with the ASIS National Auxiliary Publications Service, c/o CCM Information Sciences, Inc., 22 W. 34th St., New York 10001 and may be obtained for \$1.00 for microfiche or \$3.00 for photocopies.

$R = V_d/V_c$
 $r = (\rho C_p)_d/(\rho C_p)_c$
 S = defined by Equation (20)
 t = temperature, °C.
 V = superficial velocity of liquid, cc./sq. cm.(sec.)
 v_D = volume of drop, cc.
 z = distance along wake shedding zone, cm.

Greek Letters

α = defined by Equation (19), cm.⁻¹
 θ = dimensionless concentration
 Θ_b = defined by Equation (24)
 ρ = density, g./cc.

Subscripts

c = continuous phase
 d = dispersed phase
 i = at inlet
 l = at top of wake shedding zone
 o = at outlet
 s = at bottom of wake shedding zone
 w = wake
 z = at any point along the wake shedding zone

Superscript

* = at equilibrium

LITERATURE CITED

- Appel, F. J., and J. C. Elgin, *Ind. Eng. Chem.*, **29**, 451 (1937).
- Baird, M. H. I., M. G. Senior, and R. J. Thompson, *Chem. Eng. Sci.*, **22**, 551 (1967).
- Cavers, S. D., and J. E. Ewanchyna, *Can. J. Chem. Eng.*, **35**, 113 (1957).
- Crittendon, E. D., and A. N. Hixon, *Ind. Eng. Chem.*, **46**, 265 (1954).
- Elgin, J. C., and F. M. Browning, *Trans. Am. Inst. Chem. Eng.*, **31**, 639 (1935).
- Fleming, J. F., and H. F. Johnson, *Chem. Eng. Progr.*, **49**, 497 (1953).

- Garner, F. H., and M. Tayeban, *Anales Real Soc. Espan. Fis. Quim. Ser. B*, **56**, 479 (1960).
- Geankoplis, C. J., and A. N. Hixon, *Ind. Eng. Chem.*, **42**, 1141 (1951).
- Geankoplis, C. J., P. L. Wells, and E. L. Hawk, *ibid.*, **43**, 1848 (1951).
- Gier, T. E., and J. O. Hougen, *ibid.*, **45**, 1362 (1953).
- Hanson, Carl, *Chem. Eng.*, **75**(18), 76 (1968).
- Hendrix, C. D., S. B. Dave, and H. F. Johnson, *AIChE J.*, **13**, 1072 (1967).
- Johnson, H. F., and Harding Bliss, *Trans. Am. Inst. Chem. Eng.*, **42**, 331 (1946).
- Kreager, R. M., and C. J. Geankoplis, *Ind. Eng. Chem.*, **45**, 2156 (1953).
- Kylander, R. L., and L. Garwin, *Chem. Eng. Progr.*, **47**, 186 (1951).
- Laddha, G. S., and J. M. Smith, *ibid.*, **46**, 195 (1950).
- Letan, Ruth, and Ephraim Kehat, *AIChE J.*, **11**, 804 (1965).
- Ibid.*, **13**, 443 (1967).
- Ibid.*, **14**, 398 (1968).
- Ibid.*, **16**, 955 (1970).
- Magarvey, R. H., and R. L. Bishop, *Can. J. Phys.*, **39**, 1418 (1961).
- Magarvey, R. H., and C. S. MacLachy, *AIChE J.*, **14**, 260 (1968).
- Morello, V. S., and N. Poffenberger, *Ind. Eng. Chem.*, **42**, 1201 (1950).
- Perry, J. H., ed., "Chemical Engineering Handbook," 4th edit., pp. 14-15, McGraw-Hill, New York (1963).
- Row, S. B., J. H. Koffolt, and J. R. Withrow, *Trans. Am. Inst. Chem. Eng.*, **37**, 559 (1941).
- Ruby, C. L., and J. C. Elgin, *Chem. Eng. Progr. Symp. Ser. No. 16*, **51**, 17 (1955).
- Seidell, A., "Solubilities of Organic Compounds," 3rd edit., Vol. 2, p. 112, Van Nostrand, New York (1941).
- Sherwood, T. K., J. E. Evans, and J. V. A. Longcor, *Ind. Eng. Chem.*, **31**, 1144 (1939).
- Shih, C., and R. R. Kraybill, *Ind. Eng. Chem. Process Design Develop.*, **5**, 260 (1966).
- Vogt, H. J., and C. J. Geankoplis, *Ind. Eng. Chem.*, **45**, 2219 (1953).
- Ibid.*, **46**, 1763 (1954).
- Winnikow, S., and B. T. Chao, *Phys. Fluids*, **9**, 50 (1966).

Manuscript received March 27, 1969; revision received August 25, 1969; paper accepted August 29, 1969.

Turbulent Flow of Dilute Polymer Solutions Through an Annulus

HILLEL RUBIN and CHAIM ELATA

Israel Institute of Technology, Haifa, Israel

A semiempirical analysis of the turbulent flow of dilute polymer solutions through an annulus between two coaxial tubes is presented. This analysis is based upon the assumption that the velocity profile is logarithmic in the turbulent region. The thickness of the laminar boundary sublayer is changed by adding polymers to the solvent; this change is different at each wall of the annulus. A series of experiments was conducted in an annular system. The experimental results fit the theoretical predictions quite well.

Axial flow between concentric tubes is often encountered in heat exchangers in which heat is transferred between two fluids flowing turbulently through the annular space and the inner tube.

Major changes in the characteristics of turbulent flow may be effected by adding minute quantities of high molec-

ular polymers to a liquid. This phenomenon, which has been studied recently in turbulent pipe flow, may also generate drastic changes in the characteristics of annular flow. The potential practical importance of this phenomenon has led us to investigate the turbulent flow of dilute polymer solutions in a concentric smooth annulus.